A reference map of the human proinsulin biosynthetic interaction network

Authors: Duc T. Tran*[1], Anita Pottekat*[3,9], Saiful A. Mir[1,10], Insook Jang[3], Salvatore Loguercio[4], Alexandre Rosa Campos[8], Reyhaneh Lahmy[1,11], Ming Liu[6,7], Peter Arvan[6], William E. Balch[4,5], Randal J. Kaufman[1], Pamela Itkin-Ansari[1,2]

*** Co-authors**

[1] Development, Aging and Regeneration program, Sanford Burnham Prebys Medical Discovery Institute, La Jolla, USA

[2] Department of Pediatrics, University of California, San Diego, La Jolla, CA 92093, USA

[3] Degenerative Diseases Program, Sanford Burnham Prebys Medical Discovery Institute, La Jolla, USA

[4] The Scripps Research Institute, Department of Molecular Medicine, 10550 North Torrey Pines Rd, La Jolla, CA 92037, USA

[5] Integrative Structural and Computational Biology, The Scripps Research Institute, 10550 North Torrey Pines Road, La Jolla, CA 92037, USA

[6] Division of Metabolism, Endocrinology & Diabetes, University of Michigan Medical School, Ann Arbor, USA

[7] Department of Endocrinology and Metabolism, Tianjin Medical University, Tianjin, China

[8] Sanford Burnham Prebys Medical Discovery Institute Proteomic Core, 10901 North Torrey Pines Road, La Jolla, CA 92037, USA

[9] Current Address School of Medicine, University of California at San Diego, La Jolla, USA

[10] Current address Illumina, San Diego, CA, USA

[11] Current address OncoMed Pharmaceuticals, Inc, Redwood City, CA, USA

Corresponding:

Pamela Itkin-Ansari, PhD

Adjunct Associate Professor

Sanford Burnham Prebys Medical Discovery Institute

Joint appointment-UCSD

Tel: 858-646-3100 x 3428

Email: pitkin@sbpdiscovery.org

Abstract

The beta-cell secretory protein synthetic machinery is dedicated to insulin production, and recent reports suggest that both proinsulin misfolding and accompanying beta-cell oxidative stress could be common features in type 2 diabetes (T2D). Despite the critical role of insulin in organismal homeostasis, the precise network of interactions from early proinsulin synthesis and folding in the ER, to its subsequent trafficking through the secretory pathway, remain poorly defined. In the present study we utilized a human proinsulin-specific monoclonal antibody for affinity purification mass spectrometry, to yield unbiased profiling of the proinsulin interactome in human islets. The data reveal that human proinsulin interacts with a network of ER folding factors (including chaperones: e.g. ERDJ5, ERDJ3, GRP94, and BiP; and oxidoreductases: e.g. QSOX1, DUOX2, and PRDX4) that are remarkably conserved across both genders and 3 ethnicities. Knockdown of one of the most prominent hits, peroxiredoxin-4 (PRDX4) in MIN6 beta-cells, rendered proinsulin more susceptible to misfolding. Additionally, oxidant exposure in human islets enhanced proinsulin:BiP interactions with augmented proinsulin misfolding. Finally, oxidant exposure in human islets also led to sulfonylation of PRDX4, a modification known to inactivate peroxiredoxins. Interestingly, we observed significantly higher levels of sulfonylated (inactive) PRDX4 in islets from patients with T2D compared to that of normal islets. Taken together, these data provide a detailed reference map of the human proinsulin interaction network and suggest critical unrecognized areas for study in insulin biosynthesis, beta cell function, and T2D.

Introduction

Globally, an estimated 422 million adults are living with diabetes (http://www.who.int/en/). Moreover, diabetes and its associated complications is a growing cause of death in both developed and developing countries. A better understanding of beta cell physiology, for which failure is tightly linked to all forms of diabetes, is necessary to combat this disease. A major fraction of the beta-cell protein synthetic machinery is dedicated to the production of insulin, yet many of the proteins directly responsible for its biosynthesis remain unidentified.

Mature insulin biosynthesis begins with translocation of preproinsulin into the endoplasmic reticulum (ER) (1). Following cleavage of the signal peptide, proper proinsulin folding results in a three-dimensional structure stabilized by 3 intramolecular disulfide bonds (1). Proinsulin is transported into the Golgi complex, encounters zinc, further assembles into hexamers, and is finally transported to immature secretory granules, in which proteolytic processing enzymes cleave proinsulin to mature insulin (and C-peptide) for release in response to glucose (1).

The critical role of proinsulin folding is exemplified by rare heterozygous mutations in proinsulin that inhibit proper disulfide bond formation and folding, resulting in Mutant *INS*-gene-induced Diabetes of Youth (MIDY) both in humans and animal models (1). Global efforts applying transcriptomic, proteomic and metabolomic analyses attempted to catalog beta cell proteins that promote insulin synthesis, folding, trafficking and processing in whole human pancreatic islets identified a large number of contributing metabolic and signaling pathway components (2-5). Furthermore, murine models identified several ER resident proteins that contribute to proper proinsulin folding and processing, notably BiP, GRP170 and PDIA1 (6). Collectively, these studies indicate that proinsulin maturation is regulated by chaperones and catalyzed by ER oxidoreductases and upstream oxidases such as Ero1 (which generates stoichiometric amounts of H_2O_2 for every disulfide bond produced). Although these data provide insight into islet biology, the precise complement of folding machinery that directs proinsulin maturation — the central axis linked to beta cell function — has yet to be uncovered.

It is increasingly appreciated that a portion of proinsulin misfolds even in normal islets (7). Misfolded proinsulin activates the unfolded protein response (UPR) signaled through two protein kinases PERK and IRE1 and the transcription factor ATF6 (6). The three UPR signaling pathways each adapt the beta cell ER to prevent further accumulation of misfolded proinsulin by attenuating proinsulin synthesis, inducing expression of genes that promote translocation, folding and trafficking in the ER and activating genes that encode functions that eliminate misfolded proinsulin through Endoplasmic Reticulum Associated Protein Degradation (ERAD). If the UPR cannot restore proper proinsulin folding, beta cells undergo oxidative stress and apoptosis. Only the cohort of properly folded proinsulin molecules can transit to the Golgi from which secretory granules are formed. Beta cell stresses associated with Type I and Type II diabetes, e.g. inflammation and oxidative stress, may contribute to proinsulin misfolding (7) thereby limiting the size of the properly-folded proinsulin population and activating the UPR. Early in progression to diabetes, the UPR adapts the ER to accommodate ever-increasing proinsulin synthesis. Defects in the biosynthetic network (for folding, processing, trafficking, and exocytosis) can lead to fulminant beta cell failure (8; 9). Therefore, it is critical to better understand the cellular components that improve human beta cell insulin homeostasis and how they are maintained in the presence of extracellular insults (10).

Here we used an unbiased affinity purification mass spectrometry (AP-MS) approach to identify the machinery responsible for the central hub of human beta cell proinsulin folding. By focusing specifically on proinsulin interactions, we are able to generate beta-cell specific data in the context of whole islets. The data reveal a rich proinsulin biosynthetic network that is

remarkably conserved across a diverse group of donors. We show that proinsulin interacting proteins include the chaperones ERDJ5, ERDJ3, GRP94, BiP and the ER oxidoreductases PRDX4 and QSOX1, DUOX2 as well as novel proteins, including GWAS candidates associated with Type 1 and Type 2 diabetes. The data provide a roadmap for functional dissection of the proinsulin biosynthetic network.

Results

Defining the Human Proinsulin Biosynthetic Interaction Network

To identify the physical interactions that define proper proinsulin synthesis we first generated a series of monoclonal antibodies to human proinsulin (**Fig S1A**) and chose a conformation specific monoclonal antibody that selectively recognizes human proinsulin by immunoprecipitation (IP) (20G11) in the presence of 1% Triton X-100, with negligible cross-reactivity to mature insulin. IP of proinsulin provides beta-cell specificity, thereby avoiding the need for islet dispersal and beta cell purification methods that can stress the cells. We demonstrated that even normal islets harbor a portion of proinsulin that is misfolded albeit at lower levels than for proinsulin mutants exhibiting severe misfolding leading to Mutant *INS*-gene-induced Diabetes of Youth (MIDY) (11). To test whether IP with 20G11 recognizes misfolded human proinsulin, HEK293 cells were transfected with human proinsulin bearing MIDY point mutations located in either the insulin B- or A- chains. 20G11 efficiently IP'ed all MIDY proinsulin mutants tested (**Fig S1C**).

Proinsulin was affinity purified from human islets using 20G11 or IgG control beads and subjected to Mass Spectrometry (AP-MS). Initially, 2 MS quantification methodologies were compared; Label Free (LF) and Tandem Mass Tag (TMT) isobaric labeling approaches (**Fig S2**). Although numerous interactors were similarly identified with both technologies, the LF technique outperformed TMT in terms of fold change separation. While the dynamic range of fold change detected by LF was as high as c.a. 16, the range of fold change detected by TMT was compressed to 1 – 2.5, as described by others (12). Based upon optimal fold change separation, we implemented LF analyses for subsequent studies.

With the goal of identifying highly conserved proinsulin interactions at the core of normal human beta cell function, we procured islet preparations from 6 donors that included Caucasian, Hispanic and African American ethnicities as well as both genders. The donors had no history of diabetes, had BMI ranging from 21 to 25.4 and had normal HbAIC (4.8%-5.5%) at the time of death (**Fig 1A**). Equal numbers of islet equivalents were lysed and IP'ed with either 20G11 or mouse IgG conjugated beads as described in Methods. Proinsulin IPs were subject to

denaturation, reduction and trypsin digestion prior to LC-MS/MS analyses [a total of 90 LC-MS/MS runs were performed on these six islet preparations with 5 – 10 technical replicates per sample (see Methods)]. All data including *.raw data file, MaxQuant *.txt search results are available online at ProteomeXchange - Dataset ID PXD014476 (http://proteomecentral.proteomexchange.org/cgi/GetDataset).

AP-MS revealed consistent proinsulin (bait) recovery across the 6 human islet samples (**Fig 1B).** Comparison of MS/MS counts for bait (proinsulin) in proinsulin IP (green) versus control IP values (red) across the 6 samples revealed remarkable consistency in the recovery of proinsulin among biological replicates suggesting little technical variability as well as similar levels of proinsulin among the islet preps and donor islet preparation. MS/MS spectra were searched against the Human Uniprot database and mass spectra were analyzed with MaxQuant software (version 1.5.5.1; normalization and statistical analyses are described further in Methods). Basically, signals were normalized using R's Loess Pair Normalization, which takes into account the biological variation among human islets. For statistical analyses, MSStats (13) was utilized to calculate a confidence score (*p*-value) for each protein based on the reproducibility of detection across samples.

To identify the most robust proinsulin interactions for network analysis, the data were stringently filtered using the following criteria; (i) Proinsulin IP/Control IP intensity ratios ≥ 2-fold, (ii) $p \leq 0.05$, and (iii) total MS/MS across six samples ≥ 10. Moreover, to be certain that identified interactors were derived from beta cells, proteins were removed from analysis if the mRNA expression in beta cell single cell mRNA profiling did not reach a minimum threshold of 1 CPM (counts per million) average across all beta cell samples (14). The resulting dataset identified 461 proteins from multiple subcellular compartments, whose functions include protein synthesis, folding, degradation, trafficking, secretory vesicle formation, and proteolytic cleavage to mature insulin, as well as proteins of unknown function. For visualization of the network, cytosolic, nuclear, and mitochondrial proteins were removed as described in (15), although they remain in the uploaded dataset, which can be found at ProteomeXchange (See above). Thus, we constructed the human proinsulin biosynthetic network (**Fig 1C**).

We used AP-Western blots to validate select interactors from multiple subcellular compartments, including Myo18A, BiP, ERDJ3, ERDJ5, ERGIC1 GRP94, PRDX4, and QSOX1. Among the most robust and novel interactors identified was the Unconventional Myosin-XVIIIa (MYO18A, MSStats p value=5.86×10^{-6}, $\log_2$FC = 3.71, 98.9^{th} percentile) **(Fig 2A and Fig. S3B**). To the best of our knowledge, Myo18A has not previously been studied in beta cells. However, it was shown that knockdown of MYO18A or GOLPH3, another Golgi protein, in HEK293 cells

arrests overall secretion nearly as completely as treatment with Brefeldin A or Golgicide A (16). It was later shown in vitro that the interaction between MYO18A and GOLPH3 is required for effective vesicle budding from the Golgi to the plasma membrane, a key step in protein secretion (17). MYO18A may link Golgi membranes to the cytoskeleton, participating in the tensile force required for vesicle budding from the Golgi (18). The finding that MYO18 interacts with proinsulin, even if indirectly, suggests a firm association (that withstands 1% Triton X-100) between proinsulin and the luminal aspect of budding Golgi membranes, as previously suggested (19).

Once inside immature granules, proinsulin undergoes 3 proteolytic cleavages. The AP-MS data captured proinsulin interactions with the proteolytic enzyme, PCSK1 (Prohormone Convertase 1), that cleaves the C-peptide/B chain junction of proinsulin. Identifying this association with high confidence (MSStat *p* value = 4.6×10^{-5}, $\log_2$FC = 1.47), provides a positive control that supports confidence in the quality of the interaction data. In contrast, Islet amyloid polypeptide (IAPP), a highly expressed beta-cell protein that is stored and co-secreted with insulin, was not identified among the proinsulin interactors, speaking to the specificity of the affinity purification.

Proinsulin interaction network is tightly correlated with ER

We recently showed that a subpopulation of proinsulin in normal human islets is misfolded within the ER, existing as disulfide-linked oligomers and higher molecular weight complexes as well as properly folded proinsulin (11). To focus on ER interactors that may regulate homeostatic proinsulin folding, we relaxed stringency in order to capture resident proteins that are likely to interact transiently or only with a (misfolded) subset of the larger population of proinsulin molecules [using ß-cell expression criteria as described above and $p \leq 0.05$, (**Fig. 2B**)]. Not surprisingly, the chaperone BiP (HspA5), which is thought to be required for productive proinsulin folding (20), was identified statistically as the most significant ER chaperone interactor with proinsulin (Figs. 1C, 2A). Direct interaction of BiP with proinsulin was shown to increase with increased proinsulin synthesis (21).

Recent studies in model organisms suggest that multiple ER oxidases may produce oxidizing equivalents for protein disulfide bond formation (22; 23), however the expression and role of these oxidases in human ß-cells remains unexplored. Here, AP-MS revealed that human proinsulin is robustly associated with Peroxiredoxin-4 (PRDX4). PRDX4 is a 2-cysteine peroxiredoxin that utilizes luminal H_2O_2 to reoxidize proteins (24). In fact, PRDX4:proinsulin interactions were among the most robust in the MS dataset ($p=4.92 \times 10^{-11}$, $\text{Log}_2\text{FC} = 6.17$, 99.6^{th} percentile) (**Fig. 2A**). Interestingly, RNA expression level of PRDX4 was shown previously to be

5-fold less abundant in pancreatic islets compared to exocrine tissue (25). According to recent Human Protein Atlas (HPA) RNA-seq data, PRDX4 is expressed at 7.5 fold less in Islets of Langerhans than in exocrine glandular cells. Furthermore, expression profile of PRDX4 protein was found to be low in islets compared to high in exocrine cells in the same study using immunohistochemistry (https://www.proteinatlas.org/ENSG00000123131-PRDX4/tissue/pancreas). This finding emphasizes the functional importance of PRDX4:proinsulin interaction despite its relatively low abundance. To validate proinsulin:PRDX4 interactions, in co-transfected HEK293 cells, we found that pull-down of Flag-tagged PRDX4 co-precipitated a major fraction of either wild type or Akita mutant proinsulin (**Fig. S3C**; conversely, pull-down of myc-tagged proinsulin co-precipitated PRDX4).

Non-reducing SDS-PAGE analysis of murine islets revealed that virtually > 90% of PRDX4 protein resides in disulfide linked PRDX4 dimers and higher molecular weight complexes (HMW), with only a small fraction as the 28kDa monomer (**Fig. 2C**). To validate the specificity of the PRDX4 HMW complexes, the islets were treated with increasing concentrations of dithiothreitol (DTT, a reducing agent) *in vivo* (**Fig. 2C**). High DTT conditions increased the PRDX4 monomer relative to HMW species, but the dimer band at 49kDa was particularly stable, consistent with previous reports (22) **(Fig 2C)**. Additionally, the presence of PRDX4 in HMW species did not require the expression of protein disulfide isomerase (PDI), as beta cell specific PDI deletion did not alter the PRDX4 HMW pattern (**Fig. 2D**), which leaves open the possibility that PRDX4 in beta cells might serve client proteins (such as proinsulin) in a PDI-independent, and potentially more direct, manner.

We recently showed that the combination of beta cell specific PDI loss and exposure to high fat diet (HFD) results in increased misfolded proinsulin (23). Indeed, PRDX4 protein expression appeared markedly increased in islets with ß-cell-specific PDI deletion and treated with HFD. Moreover, recovery of PRDX4 in high molecular weight complexes was markedly increased in HFD treated islets with ß-cell-specific PDI deletion (**Fig. 2F**). Notably, overlaying proinsulin and PRDX4 Western blots from the same membrane revealed that 2 of the 3 most prominent bands corresponding to misfolded proinsulin comigrating with the major PRDX4 bands (orange bands, **Fig 2F**).

To determine whether proinsulin folding is supported by PRDX4, we used shRNA to deplete PRDX4 in MIN6 cells, with a 64 – 75% knockdown compared to cells infected with scrambled shRNA (**Fig 3A**). In cells in which the chaperone BIP was cleaved by the bacterial toxin SubAb, PRDX4 knockdown resulted in increased proinsulin misfolding, indicating that loss of BiP increases reliance on PRDX4 as a folding factor (**Fig 3B**). The cells were then treated

with an oxidant challenge using 100 µM menadione for 1 hour. From these studies, it was apparent that PRDX4-depleted ß-cells were hypersensitive to oxidant challenge (**Fig. 3C**).

Oxidative stress is a feature of beta cells in diabetic patients, prompting examination of its effect on the oxidation of proinsulin in human islets. Indeed, oxidant challenge with menadione increased proinsulin misfolding (**Fig 4A**), despite the fact proinsulin:BiP interactions were increased **(Fig 4B)**. Moreover, menadione induced proinsulin misfolding was accompanied by sulfonylation of PRDX4 (**Fig 4A**), a modification known to inactivate the catalytic activity of PRDX4 (26). Intriguingly, examination of PRDX4 sulfonylation status in a series of untreated human islet samples from non-diabetic and diabetic sources revealed for the first time that islets from patients with T2D exhibit 3.3-fold increase in sulfonylated PRDX4 relative to total PRDX4 ($p=0.011$) (**Fig 5**).

Discussion

Significant efforts have been made to understand beta cell biology at OMICs level. One potential limitation of these studies is that they may inadvertently incorporate results from multiple cell types in the pancreas despite efforts to purify beta cells. Advances in OMICs at the single cell level are playing an important role in defining cells at the RNA level but the single cell approach remains difficult with proteins. By focusing specifically on the proinsulin folding/processing pathway, we were able to generate beta-cell specific data in the context of whole islets and thus avoided harsh conditions to disperse islets, which may alter islet physiology. To focus on synthesis and trafficking, we generated a highly specific monoclonal antibody to human proinsulin, that efficiently immunoprecipitates proinsulin with negligible reactivity to mature insulin (**Fig S1**).

The most striking feature of this data set is the tight conservation of human proinsulin biosynthetic network across 6 donors reflecting 3 ethnicities and both genders. A technical aspect that may have contributed to the data concordance was that we procured human islets from a single source to avoid artifacts due site-specific islet isolation practices.

For the network design the criteria were quite stringent, requiring at least 2 fold increase in Intensity between 20G11 IP and IgG IPs, $p<$ or $=$ to 0.05 and MS/MS counts of at least 10 among the 6 human islet preparations as well as a minimum mRNA expression level in published mRNA seq studies from single beta cells (24). Our findings corroborate the previously identified proinsulin interacting proteins, BiP (HSPA5) and GRP94 (GSP90B1) that have both been shown to play essential roles in proinsulin folding (27) while extending those studies to provide an entire interaction network.

We previously performed AP-MS to identify proinsulin and insulin interactors in murine MIN6 cells (28). Consistent with those studies, here we identified DNAJB11(ERDJ3), DNAJC6 ($p58^{IPK}$), ERP44, IQGAP2, and EIF2A as high confidence human proinsulin interacting proteins. Not surprisingly, TMEM24, that interacted more robustly with mature insulin than with proinsulin in our previous murine MIN6 study, was not identified in this study, which focused solely on proinsulin interactions in human islets. The two studies also utilized unique, species specific, antibodies, which may lead to differences in prey capture.

Among the most significant newly identified proinsulin interacting proteins was PRDX4, the only one of the 6 human PRDX proteins that is ER resident. We show in native islets that PRDX4 primarily resides in high molecular weight complexes which may include oligomers (22) but also clearly involve other proteins as not all bands are multimers of 28 kDa. Importantly, all bands collapse to PRDX4 monomer and dimer upon treatment with DTT, validating that they specifically contain PRDX4.

Although PRDX4 is not an essential ER enzyme in mice, except in testes (29), we find that proinsulin is more prone to misfolding when PRDX4 levels are low and stress is induced by BiP cleavage or oxidant treatment (**Fig 3**), indicating that under stress conditions PRDX4 plays an important role. These data are consistent with the finding that MEFs lacking ERO1 were intolerant of PRDX4 deficiency (15). The involvement of PRDX4 with the redox protein network is further emphasized by the finding that loss of QSOX1, one of our identified proinsulin interactors induces overexpression of PRDX4 in mouse hearts (30). Here we also show that loss of PDI increases expression of PRDX4 and its incorporation into high molecular weight complexes suggesting that there is also increased need for PRDX4 in the absence of PDI (25). Whether islets from PRDX4 knockout mice would also exhibit beta cell problems under stress is not known.

In yeast, it has also been suggested that the single PRDX-like protein is a molecular triage agent that absorbs oxidation to spare thioredoxin (31). It may not be surprising then that overexpression of PRDX4 in mice has been shown to repress beta-cell apoptosis, induce beta-cell proliferation and provide protection to beta-cells under stress, e.g. against streptozotocin-induced diabetes (32). Finally, PRDX4 may also play a role in signal transduction regulatory circuitry involving redox-controlled processes in the ER (33) .

We find that PRDX4 is sulfonylated in human islets when they are exposed to oxidative stress, e.g. treated with the oxidant menadione (Fig 5). Moreover, sulfonylation of PRDX4 was increased in islets from patients with T2D. The data suggest that beta cells in patients with T2D have diminished capacity to handle oxidative stress. It is intriguing that serum of patients with

T2D has higher levels of circulating PRDX4 than controls (34) although the cell source of the PRDX4 is not yet known (11; 35).

In summary, we have identified a complex set of protein-protein interactions that reflects the dynamic folding compartments dictating protein trafficking through the exocytic pathway (36; 37). The proinsulin interaction network provides a critical resource to characterize previously unknown molecular features of the beta cell secretory pathway. It will now be of interest to determine which proteins interact with proinsulin directly versus indirectly and to uncover their individual roles in promoting efficient proinsulin biosynthesis.

Methods

Cell Culture and Treatments.

Islets were procured from Prodo labs (Aliso Viejo, CA). Islet preparations averaged 85-95% purity by DTZ and 95% viability by EB/FDA staining. Each preparation was tested for glucose responsiveness prior to use. Islets were cultured in Prodo Islet Complete Media . MIN6 cells were cultured in DMEM with 4.5g/L glucose and L-glutamine, 3.4% $NaHCO_3$, 1X penicillin, streptomycin, 275 nM β-mercaptoethanol (BME), 15% FBS. Cells were treated with menadione (100 µM, 1 hr), SubAb (2 µg/mL, 2 hrs), mutant SubAb (2 µg/mL, 2 hrs). After treatment, cells were washed once with PBS. Islets were typically lysed in RIPA or Lysis Buffer as described below. MIN6 cells were lysed directly in 2X Laemmli without BME, heated at 100 ^{o}C for 10 mins and clarified by centrifugation at 17,000 g for 15 minutes. For reducing samples, BME was added to lysate aliquots to 2.5% and heated again at 100^{o}C for 10 mins before SDS-PAGE.

Immunoprecipitation of Proinsulin from Human Islets for mass spectrometry analyses

Human islets were lysed in lysis buffer (50mM Tris pH7.4, 150mM NaCl and 1% TX-100, and 1X protease inhibitor cocktail (Thermo Scientific Pierce)) on ice for 45 min. For each IP used in MS, lysates were pre-cleared with Protein G beads. Lysate was immunoprecipitated with beads crosslinked to mouse IgG or proinsulin antibody (20G11) overnight at 4°C and then washed twice with lysis buffer and once with lysis buffer without detergent. A fraction of the beads was removed for protein elution to confirm successful IP by western blot and silver staining. The majority of the beads were subjected to denaturation, reduction and trypsin digestion followed by Mass spectrometry analysis.

Mass spectrometry sample preparation

Proteins were digested in 8M urea 50 mM ammonium bicarbonate buffer. Briefly, cysteine disulfide bonds were reduced with 5 mM tris(2-carboxyethyl)phosphine (TCEP) at 30°C for 60 min followed by cysteine alkylation with 15 mM iodoacetamide (IAA) in the dark at room temperature for 30 min. Following alkylation, urea was diluted to 1 M using 50 mM ammonium bicarbonate, and proteins were finally subjected to overnight digestion with mass spec grade Trypsin/Lys-C mix (Promega, Madison, WI). Digested proteins were finally desalted using a C18 TopTip (PolyLC, Columbia, MD) according to the manufacturer's recommendation), and the organic solvent was removed in a SpeedVac concentrator prior to LC-MS/MS analysis. To label samples with TMT for TMT vs. LF comparison, TMTsixplex™ Isobaric Label kit (ThermoFisher Scientific) was used according to manufacture protocol.

2D LC-MS/MS analysis

For 3 out of 6 islet batches, islets were divided into four equal parts based on number of islet equivalents, one of which was immunoprecipitated with mouse IgG as a control, and the other three with the proinsulin specific antibody 20G11 as three experimental replicates. Prior to MS/MS analyses, three experimental replicates of 20G11 IP were pooled together resulting in a total of 2 samples. Each sample was subject to state of the art 2 Dimensional LC-MS/MS analysis in which the peptide mixture was first separated in a high-pH reverse phase chromatography into 5 fractions before directly subject to a second low-pH reverse phase chromatography coupled with MS/MS analyses. This analysis results in 5 technical replicates per sample and a total of 30 LC-MS/MS runs. For the other 3 islet batches, islets were also divided into four equal parts, two of which was precipitated with IgG as a control and the other with 20G11. Each experimental replicate was analyzed separately in LC-MS/MS analysis resulting in a total of 60 runs with 10 technical replicates per sample.

Dried samples were reconstituted in 100mM ammonium formate pH ~10 and analyzed by 2DLC-MS/MS using a 2D nanoACQUITY Ultra Performance Liquid Chromatography (UPLC) system (Waters corp., Milford, MA) coupled to an Orbitrap Velos Pro mass spectrometer (Thermo Fisher Scientific). Peptides were loaded onto the first dimension column, XBridge BEH130 C18 NanoEase (300 µm x 50 mm, 5 µm) equilibrated with solvent A (20mM ammonium formate pH 10, first dimension pump) at 2 µL/min. The first fraction was eluted from the first dimension column at 17% of solvent B (100% acetonitrile) for 4 min and transferred to the second dimension Symmetry C18 trap column 0.180 x 20 mm (Waters corp., Milford, MA) using a 1:10 dilution with 99.9% second dimensional pump solvent A (0.1% formic acid in water) at 20 µL/min. Peptides were then eluted from the trap column and resolved on the analytical C18 BEH130 PicoChip

column 0.075 x 100 mm, 1.7µm particles (NewObjective, MA) at low pH by increasing the composition of solvent B (100% acetonitrile) from 2 to 26% over 94 min at 400 nL/min. Subsequent fractions were carried with increasing concentrations of solvent B. The following 4 first dimension fractions were eluted at 19.5, 22, 26, and 65% solvent B. The mass spectrometer was operated in positive data-dependent acquisition mode. MS1 spectra were measured with a resolution of 60,000, an AGC target of 10^6 and a mass range from 350 to 1400 m/z. Up to 5 MS2 spectra per duty cycle were triggered, fragmented by CID, with an AGC target of 10^4, an isolation window of 2.0 m/z and a normalized collision energy of 35. Dynamic exclusion was enabled with duration of 20 sec.

Mass Spectrometry Data Processing

All mass spectra from were analyzed with MaxQuant software version 1.5.5.1. MS/MS spectra were searched against the Homo sapiens Uniprot protein sequence database (version January 2015) and GPM cRAP sequences (commonly known protein contaminants). Precursor mass tolerance was set to 20ppm and 4.5ppm for the first search where initial mass recalibration was completed and for the main search, respectively. Product ions were searched with a mass tolerance 0.5 Da. The maximum precursor ion charge state used for searching was 7. Carbamidomethylation of cysteines was searched as a fixed modification, while oxidation of methionines and acetylation of protein N-terminal were searched as variable modifications. Enzyme was set to trypsin in a specific mode and a maximum of two missed cleavages was allowed for searching. The target-decoy-based false discovery rate (FDR) filter for spectrum and protein identification was set to 1%. Note that proinsulin is searched as insulin in the database.

Normalization

Intensity of each identified peptide was subtracted from the control IP and Log_2Fold Change (Log_2FC) was calculated. Two different methods of Mass Spectrometry analysis, Label Free and Tandem Mass Tag (TMT) isobaric labeling analysis were employed for a single islet prep (HP 15157-01) to compare the two methods (**Figure S2**). Based on resolution of fold changes, Label Free (LF) analyses were implemented for all of the samples.

For normalization, Loess Global vs Pair, quantile, MAD and Total Intensity methods were compared. Preliminary evaluation of the most suitable normalization method for the IP-MS data (Loess-R) was conducted with Normalyzer (38). Although outcomes looked very similar with all of these methods Loess Pair gave the best normalized dataset as the method considers control and sample within each experiment separately rather than averaging samples and controls across

subjects. This is most suited for human islets given the possibility of variations from one human subject to another.

Statistical Analysis

For Statistical analysis, the datasets were analyzed by two methods (1) SAINT (Significance Analysis of INTeractome) analysis (13; 39) or MSStats (13) to score and evaluate confidence of interactions in proinsulin IPs versus the control IgG coated beads. SAINT is a computational tool that assigns unbiased confidence scores to protein-protein interaction data whereas MSStats calculates Fold change and allows one to extract a confidence score (p-value) for each protein based on the reproducibility of detection across samples. Due to a large dynamic range in the demographics of our islet donors, MSStats was chosen as this open source R based platform tool enables better quantitation of the sources of variations (40).

Final list of proinsulin interactome was selected to have (i) Fold Change (Ins vs. Control) ≥2, (ii) p-value ≤ 0.05 and (iii) deltaMS/MS (total sum of spectral counts across replicates) ≥ 10. Additional filtering was performed using previously published single cell RNA-seq data (24) to generate list of genes that were “at least expressed in Beta-cells”. The threshold was set to 1 CPM (counts per million) average across all beta cell samples yielding ~13K genes out of 20K.

Bioinformatic Analyses

Initial proteostasis compartment analysis was comprised of unbiased and curated data as shown at https://github.com/balchlab/PPT_annotation. Pathway and process enrichment analysis were carried out with the following ontology sources: KEGG Pathway, GO Biological Processes, Reactome Gene Sets and CORUM. Gene annotation and analysis resources included Metascape (41) and Enrichr (42). Protein Atlas (43) was used as primary source for subcellular localization, protein function and proteostasis classification.

Next, GWAS candidate genes and regions for T1D were gathered from the ImmunoBase resource (www.immunobase.org) - currently, 55 validated GWAS genes and 1090 genes in GWAS regions, and set out to connect T1D GWAS genes to Insulin interacting proteins through human protein-protein interactions. In particular, the Human Integrated Protein-Protein Interaction Reference database (44) was used as source of PPI data - incorporating interaction data from major expert-curated experimental PPI databases (such as BioGRID, HPRD, IntAct and MINT). Our network methods included Network Propagation (45) for amplification of biological signal, Prize-collecting Steiner Trees (46) to detect hidden components within the underlying regulatory

and signaling network, and Network-augmented Genomic Analysis (NAGA) (47) to detect a compact network of nodes involved in shortest paths between GWAS genes and Proinsulin. R/Bioconductor, in particular the igraph library, was used for network manipulation, data integration and analysis, and Cytoscape (48) for interactive network visualization and presentation.

Finally, a prioritization table was assembled based on all above information, in which, for each Proinsulin-interacting protein, the following data was reported: (i) binding to proinsulin (as Fold Change (Ins vs. Control)), (ii) scores from the above PPI network-based methods for integrating T1D GWAS genes, (iii) subcellular localization, (iv) biological function, (v) Proteostasis classification. The proteins were ranked in the table based on a consensus score obtained from the ensemble of network methods. Subcellular localization and proteostasis annotation were used to assess the biological plausibility of potential top scoring candidates.

Mice and Murine Islet Isolation

All mice models used in this experiment were made as reported elsewhere (23). In brief, mice with PDIA1 floxed alleles were obtained from Dr. J. Cho (Univ. of Illinois-Chicago) and crossed with Rat Insulin Promoter (RIP)-CreER transgenic mice. PDIA1 deletion was performed by IP injection of the estrogen receptor antagonist Tamoxifen (Tam) (4mg/mouse) three times a week. Male mice were pair-housed for the high fat diet (HFD) study. All procedures were performed by protocols and guidelines reviewed and approved by the Institutional Animal Care and Use Committee (IACUC) at the SBP Medical Discovery Institute. Murine islets were isolated by collagenase P (Roche) perfusion as described following by histopaque-1077 (Sigma-Aldrich, Inc. St. Louis) gradient purification. Islets were handpicked and studied directly or after overnight culture in RPMI 1640 medium (Corning 10-040-CV) supplemented with 10% FBS, 1% penicillin/streptomycin, 100µg/ml primocin, 10mM Hepes, and 1mM sodium pyruvate.

Validation of proinsulin interactions

For proinsulin interactions validated in human islets 2500 IEQ of normal human islets were lysed in 50mM Tris pH7.4, 150mM NaCl and 1% TX-100, 1X PMSF, 1X protease inhibitor cocktail and 1X phosphatase inhibitor cocktail (Thermo Scientific Pierce) on ice for 30 min. Lysates were precleared with protein A/G Agarose beads at 4^{o}C for 1 hr before 132 µg of total protein extracts from human islet lysate with 132 µg of either proinsulin specific primary antibody (20G11) or mouse IgG Fc portion overnight at 4^{o}C. Antibody bound proinsulin and its interactors were captured by binding to 100 µL of protein A agarose beads suspension 4 hrs (RT). Unbound

supernatant was saved, and beads were washed with lysis buffer without detergent (1 x 100 µL and 1 x 500 µL) prior to eluting in 50 µL of 2X Laemmli buffer at 100ºC for 10 min. 5% of either Lysate and Supernatant were run along with 12% of Elution (IP).

For proinsulin interactions validated in HEK293 cells, cells were plated in 6 or 12 well plates the day prior to transfection. Plasmids expressing human PRDX4-FLAG and Human QSOX1-HA were purchased from Sino Biological Inc. (Wayne, PA). Vectors expressing WT or Akita mutant c-Myc tagged hProins were obtained from Peter Arvan at University of Michigan (49). 2µg total DNA was transfected using Viafect transfection reagent following manufacturer instructions. PCDNA3.1 vector was used as the control and to match total amount DNA for co-transfection experiments. After 48 hours of transfection, cells were harvested, and protein was extracted with a lysis buffer on ice for 15-20 min. Supernatant was collected after spinning samples at 14000 rpm for 10 min at 4ºC. Protein concentration was estimated by DC protein assay method (Biorad). Immunoprecipitation of tagged proinsulin, PRDX4 or QSOX1 was performed using agarose beads conjugated with anti-MYC, FLAG or HA respectively according to manufacturer protocol (Pierce). Freshly prepared lysates (250-350 µg total protein) were used for immunoprecipitation of c-Myc-Tag human proinsulin with c-Myc-Tag antibody coated magnetic beads using Magnetic c-Myc-Tag IP/Co-IP Kit (Pierce# 88844). Lysates were mixed with 25-50µl magnetic beads and incubated for 45 min at RT with mixing. After the incubation, supernatant was saved for analysis and after washing the beads, samples were eluted in 100µl of 1X non-reducing western blotting sample buffer. IP samples were reduced with DTT/ BME before separating onto the gel.

Western blotting

Samples were prepared in Laemmli sample buffer without (non-reducing) or with (reducing) 2.5% BME. After boiling for 10 min at 100ºC, samples were analyzed by SDS-PAGE (either 4-20% Tris-glycine or 4-12% Bis-tris pre-cast gel, Bio-rad Laboratories, Inc.) and transferred to nitrocellulose membranes (Bio-rad Laboratories, Inc.). Membranes were blocked with 5% BSA (4ºC, 1hr) and cut according to molecular weight markers and incubated with corresponding primary antibodies (4ºC, O.N): Rabbit BiP (for human islets), Rabbit GRP94 (Cell Signaling Tech, Danvers, MA), or Rabbit ERDJ5, Rabbit ERGIC1, Rabbit Myo18A and ERDJ3 (ProteinTech, Rosemont, IL), Goat PRDX4 (R&D System, Minneapolis, MN), Mouse 20G11 (generated in house), HA and C-MYC (Abcam, Cambridge, MA). On murine islets, Rabbit vinculin (Proteintech, 66305-1-lg), Rabbit PDIA1 (Proteintech, 11245-1-AP), Mouse proinsulin (HyTest Ltd., 2PR8, CCI-17), and Rabbit BiP (for MIN6 cells, a kind gift from Dr Hendershot). For

secondary antibodies, goat anti-mouse, goat anti-rabbit, donkey anti goat and donkey anti-guinea pig antibodies were used in 1:5000 (Li-Cor, IRDye®-800CW or IRDye®-680RD). After wash, membranes were imaged on Licor Odyssey CLX set up and western blot images were analyzed by ImageJ for quantitation of band intensity.

PRDX4 knockdown

Viral vectors expressing lentiviral particles with 4 unique 29mer target-specific shRNA (A/B/C/D) to murine PRDX4 and 1 scramble control (non-specific or NS) were purchased from Origene (Rockville, MD). MIN6 cells were seeded on 48 well plates and cultured overnight in 0.3 mL medium. Polybrene (1mg/mL) was added at 1:125 ratio to culture medium before 20 µL of lentiviral particles (10^7 TU/mL) was added to infect cells overnight. Infected cells were selected using Puromycin and subsequently by fluorescent activated cell sorting. For cell sorting, MIN6 cells were detached from plates using trypsin, quenched with FBS and resuspended in FACS buffer (1% FBS in PBS). Approximately 2 – 4 million cells were sorted for high GFP intensity, Cells were later transferred and maintained in MIN6 specific media (DMEM with 4.5g/L glucose and L-glutamine 3.4% $NaHCO_3$, 1X penicillin, streptomycin, 275 nM BME, 15% FBS).

Figure Legends

Figure 1. Defining the Proinsulin Biosynthetic Interaction Network.

(A) Human islets from 6 donors were used for AP-MS were procured from Prodo labs.

(B) Total MS/MS counts for Proinsulin bait (green) or IgG bait (orange) from the six islet preparations reported in (A).

(C) Network analysis of robust proinsulin protein:protein interactions generated by Cytoscape. Data were filtered for all of the following criteria (i) Proinsulin IP/Control IP intensity ratios ≥ 2fold, (ii) p ≤0.05, (iii) total MS/MS across 6 samples ≥10, and (iv) mRNA expression in single cell mRNA profiling of beta cells had to reach at least 1 CPM (counts per million). Colors indicate protein categories. The categories nuclear, mitochondria and undefined are not included.

Figure 2 PRDX4 is a robust proinsulin interactor and is induced by loss of PDI

(A) Volcano plot showing the relationship between log_2FC intensity (Proinsulin IP vs. IgG control) and p value. Ten selected robust interactors are named.

(B) List of the most robust endoplasmic reticulum (ER) resident proinsulin interactors as determined by p value ≤0.05.

(C) Lysates from untreated (0) murine islets or islets treated with a gradient of DTT concentrations ranging from 1 to 15 mM were run on a non-reducing gel and blotted for PRDX4. Quantification of disulfide linked HMW complex (size indicated 49 – 198 kDa) and PRDX4 monomer (28 kDa) intensity was also shown (bottom graph).

(D) Islets from normal (PDIA1 fl/+ and PDIA1 fl/fl) mice versus PDI knockout female mice (PDIA1 fl/fl; Cre) were lysed, analyzed on non-reducing and reducing gel and blotted for PRDX4. Quantification of PRDX4 normalized by previously published vinculin (Ref (23) Fig 1C&D) was shown in accompanying graph (right). Beta-cell specific loss of PDIA1 modestly increases PRDX4 expression but does not change PRDX4 incorporation into high molecular weight complexes.

(E) Male mice, with and with PDI ko, were fed a high fat diet (HFD) and isolated islets were treated +/- menadione. Reducing gels for PRDX4 and vinculin indicate that loss of PDIA1 increased PRDX4 expression (lanes 1 and 5 versus 3 and 7) with or without menadione treatment (lanes 1 and 5 versus 2 and 6, and lanes 3 and 7 versus 4 and 8).

(F) Islet preps from (E) were analyzed on a single non-reducing gel. Blotting for proinsulin showed that beta cell specific loss of PDI in mice on HFD increased proinsulin in high molecular weight complexes (lanes 1 and 5 versus 3 and 7) and menadione treatment increased proinsulin in high molecular weight complexes in both WT and (fl/+) and KO mice (as we recently reported (23)). The membrane was stripped and reblotted for PRDX4. Imagej was used to merge the two non-reducing blots together revealing co-localization of multiple major bands in proinsulin and PRDX4 blots, two of which were highlighted by arrows. Note the stripped membrane gave similar results to blots run separately.

Figure 3 Loss of PRDX4 exacerbates proinsulin misfolding induced by BiP cleavage or oxidative stress in MIN6 cell lines.

(A) Knockdown of PRDX4 with 2 independent shRNAs is shown with accompanying graph showing PRDX4 level normalized to GAPDH loading control.

(B) MIN6 cell line expressing shRNA (i.e. C) specific to PRDX4 and one with a non-specific shRNA (NS) were challenged with SubAb (2 µg/mL, 2 hrs), a perturbagen that specifically cleaves BiP or with mutant SubAb (2 µg/mL, 2 hrs), its enzymatically inactive counterpart. Non-reducing gel (Upper panel) blotted for mouse proinsulin NS. Accompanying graphs

(upper right) showed quantification of HMW bands from 14 kDa and up normalized in 2 different ways by vinculin or total proinsulin. Bottom panels showed total proinsulin, BIP and two loading controls (vinculin and GAPDH) in parallel reducing gel. The effect of SubAb on abundances of BiP is clear, which also results in small decrease in total Proinsulin.

(C) MIN6 cell lines with PRDX4 knockdown (shRNAs C and D), and the NS line were treated with menadione (100 µM, 1 hr). Non-reducing gel blotted with mouse proinsulin displayed a similar mild increase of HMW complexes in the PRDX4 knock down compared to NS. Bottom panels showed the dark exposure of non-reducing proinsulin monomer and loading control (Vinculin, GAPDH) along with total Proinsulin, and Insulin in accompanying reducing gel. Accompanying graphs (upper right) showed quantification of HMW bands from 14 kDa and up normalized in 2 different ways by vinculin or total proinsulin.

Figure 4 Oxidant **(**Menadione) treatment of human islets induces proinsulin misfolding, increased proinsulin:BiP interactions and PRDX4 sulfonylation.

(A) Non-reducing gels (upper panels) of human islet samples treated with Menadione (100 µM, hr), Cytokines (50 U/mL IL1β, 1000 U/mL IFN-γ, 48 hrs) or untreated (CtrL) and blotted for human proinsulin, PRDX4 or sulfonylated prdxs (prdx-SO_3). Bottom panels display reducing gels for corresponding levels of total proinsulin, PRDX4 of prdx-SO_3 and loading control (vinculin).

(B) Proinsulin immunoprecipitation of samples in (A) reveals proinsulin:BiP interactions across all treatments. Interaction was specific for proinsulin immunoprecipitation compared to mouse IgG. Note that the BIP band was not observed in sample that contains only antibody with no lysate (No Lys). Normalization of the ratios of BIP immunoprecipitated by proinsulin versus IgG reveals increased BIP: proinsulin in the presence of menadione (graph).

Figure 5 T2D islets trend to high molecular proinsulin complexes relative to monomer and exhibit increased PRDX4 sulfonylation.

(A) Non-reducing gels (upper panel) of human islet preparations from 4 individual normal and 4 Type 2 Diabetic (T2D) islet preparations normalized by total protein concentration determined by Lowry assay and blotted for human proinsulin. Reducing gels for total proinsulin and loading control (GAPDH) are shown (bottom panels). Quantification of

HMW band intensity normalized by i) proinsulin monomer on the non-reducing, or ii) total proinsulin on reducing gel normalized to loading control (GAPDH).

(B) A reducing gel for samples in (A) was blotted for both PRDX4 (green) and sulfonylated prdxs (i.e. prdx-SO_3, red). Merged image showed co-localization of PRDX4 band with its sulfonylated version at the same molecular weight. Intensity of the sulfonylated PRDX4 band (yellow arrow) was quantified and averaged across all islet preparations, showing a clear increase of sulfonylated PRDX4 in T2D versus normal islets.

Figure S1 - Antibody Generation and Validation. Specificity of monoclonal antibodies to proinsulin for proinsulin. (A, B) Immunoblot of lysates from murine MIN6 cells, rat INS-1 cells and human islets with in-house generated monoclonal antibodies. C) WT proinsulin and proinsulin MIDY mutants were overexpressed in COS1 cells and immunoprecipitated with 20G11 antibody.

Figure S2 - Comparison of Label Free and TMT Mass Spectrometric analysis on one islet preparation (HP-15157-01) identified common proteins but with different sensitivities.

Figure S3. Validate MS/MS Interactions by AP-western blot

(A) Validation of BiP, ERDJ5, GRP94 and ERGIC1 interaction with proinsulin was performed by immunoprecipitation of 132 µg of total protein extracts from human islet lysate (HP-19038-01) with 132 µg of either proinsulin specific primary antibody (20G11) or mouse IgG Fc portion overnight at 4^{o}C. Antibody bound proinsulin and its interactors were captured by binding to 100 µL of protein G agarose beads at room temperature for 4 hrs. Unbound supernatant (sup) were saved and beads were washed with lysis buffer without detergent (1 x 100 µL and 1 x 500 µL) prior to eluting in 50 µL of 2X Laemmli buffer at 100^{o}C for 10 min. 5% either Lysate and Supernatant (Sup) were run along with 12% of Elution (IP). Membranes were cut according to molecular weight markers and blotted for the indicated primary antibodies: Rabbit BIP, ERDJ5, GRP94 and ERGIC1.

(B) Validation of Myo18A, BiP, and ERDJ3 interaction with proinsulin was performed by immunoprecipitation of lysates from a different human islet sample (HP-19038-01) in similar manner. Negative control was an immunoprecipitation where no lysate (No Lys) was added. 4% either Lysate and 12 of Elution (IP) was analyzed on reducing gels. Membranes were cut according to molecular weight markers and blotted for the indicated primary antibodies: Rabbit Myo18A, BIP, ERDJ3.

(C) PRDX4 expression in human islet preparations. Plasmids carrying human PRDX4-FLAG-Tag and/or hProins-c-Myc-Tag, and/ or PCDNA control plasmid were transiently

transfected into HEK293 cells followed by immunoprecipitation with MYC-beads or FLAG beads. Lysates 5%, IPs 15% and supernatants 5% were blotted for PRDX4, FLAG, human proinsulin (20G11) and c-MYC.

(D) Proinsulin Interaction with QSOX-1 and Myo18A. Plasmids carrying human QSOX1-HA-Tag and/or hProins-c-Myc-Tag or PCDNA control plasmid were transiently transfected into HEK293 cells followed by immunoprecipitation with MYC-beads (upper panel) or HA beads (lower panel). Lysates 5%, IPs 15% and supernatants 5% were blotted for HA (QSOX1) human proinsulin (20G11) and MYC tag (upper panel)

Figure S4. PRDX4 expression vs PDX1 expression in human beta cell single cell RNAseq (12).

REFERENCES:

1. Liu M, Weiss MA, Arunagiri A, Yong J, Rege N, Sun J, Haataja L, Kaufman RJ, Arvan P: Biosynthesis, structure, and folding of the insulin precursor protein. Diabetes, Obesity and Metabolism 2018;20:28-50
2. Waanders LF, Chwalek K, Monetti M, Kumar C, Lammert E, Mann M: Quantitative proteomic analysis of single pancreatic islets. Proceedings of the National Academy of Sciences 2009;106:18902-18907
3. Ahmed M, Forsberg J, Bergsten P: Protein profiling of human pancreatic islets by two-dimensional gel electrophoresis and mass spectrometry. Journal of proteome research 2005;4:931-940
4. Schrimpe-Rutledge AC, Fontes G, Gritsenko MA, Norbeck AD, Anderson DJ, Waters KM, Adkins JN, Smith RD, Poitout V, Metz TO: Discovery of novel glucose-regulated proteins in isolated human pancreatic islets using LC-MS/MS-based proteomics. Journal of proteome research 2012;11:3520-3532
5. Zhang L, Lanzoni G, Battarra M, Inverardi L, Zhang Q: Proteomic profiling of human islets collected from frozen pancreata using laser capture microdissection. Journal of proteomics 2017;150:149-159
6. Scheuner D, Kaufman RJ: The unfolded protein response: a pathway that links insulin demand with β-cell failure and diabetes. Endocrine reviews 2008;29:317-333
7. Arunagiri A, Haataja L, Pottekat A, Pamenan F, Kim S, Zeltser LM, Paton AW, Paton JC, Tsai B, Itkin-Ansari P: Proinsulin misfolding is an early event in the progression to type 2 diabetes. eLife 2019;8:e44532
8. Lu M, Lawrence DA, Marsters S, Acosta-Alvear D, Kimmig P, Mendez AS, Paton AW, Paton JC, Walter P, Ashkenazi A: Opposing unfolded-protein-response signals converge on death receptor 5 to control apoptosis. Science 2014;345:98-101
9. Roth DM, Hutt DM, Tong J, Bouchecareih M, Page L, Wang N, Seeley T, Dekkers JF, Beekman JM, Garza D, Miller J, Masliah E, Morimoto RI, Balch WE: Modulation of the maladaptive stress response to mange diseases of protein folding. PloS Biol 2014;Submitted under final review
10. Back SH, Kaufman RJ: Endoplasmic reticulum stress and type 2 diabetes. Annual review of biochemistry 2012;81:767-793
11. Liu M, Hodish I, Rhodes CJ, Arvan P: Proinsulin maturation, misfolding, and proteotoxicity. Proceedings of the National Academy of Sciences 2007;104:15841-15846
12. Megger DA, Pott LL, Ahrens M, Padden J, Bracht T, Kuhlmann K, Eisenacher M, Meyer HE, Sitek B: Comparison of label-free and label-based strategies for proteome analysis of hepatoma cell lines. Biochimica et Biophysica Acta (BBA)-Proteins and Proteomics 2014;1844:967-976
13. Choi M, Chang C-Y, Clough T, Broudy D, Killeen T, MacLean B, Vitek O: MSstats: an R package for statistical analysis of quantitative mass spectrometry-based proteomic experiments. Bioinformatics 2014;30:2524-2526
14. Wang YJ, Schug J, Won K-J, Liu C, Naji A, Avrahami D, Golson ML, Kaestner KH: Single-cell transcriptomics of the human endocrine pancreas. Diabetes 2016;65:3028-3038
15. Zito E, Melo EP, Yang Y, Wahlander Å, Neubert TA, Ron D: Oxidative protein folding by an endoplasmic reticulum-localized peroxiredoxin. Molecular cell 2010;40:787-797
16. Ng MM, Dippold HC, Buschman MD, Noakes CJ, Field SJ: GOLPH3L antagonizes GOLPH3 to determine Golgi morphology. Molecular biology of the cell 2013;24:796-808
17. Rahajeng J, Kuna RS, Makowski SL, Tran TT, Buschman MD, Li S, Cheng N, Ng MM, Field SJ: Efficient Golgi Forward Trafficking Requires GOLPH3-Driven, PI4P-Dependent Membrane Curvature. Developmental cell 2019;
18. Taft MH, Behrmann E, Munske-Weidemann L-C, Thiel C, Raunser S, Manstein DJ: Functional characterization of human myosin-18A and its interaction with F-actin and GOLPH3. Journal of Biological Chemistry 2013;288:30029-30041
19. Orci L, Ravazzola M, Perrelet A: (Pro)insulin associates with Golgi membranes of pancreatic B cells. PNAS 1984;81:6743-6746

20. Wu J, Kaufman R: From acute ER stress to physiological roles of the unfolded protein response. Cell death and differentiation 2006;13:374
21. Scheuner D, Vander Mierde D, Song B, Flamez D, Creemers JW, Tsukamoto K, Ribick M, Schuit FC, Kaufman RJ: Control of mRNA translation preserves endoplasmic reticulum function in beta cells and maintains glucose homeostasis. Nature medicine 2005;11:757
22. Tavender TJ, Springate JJ, Bulleid NJ: Recycling of peroxiredoxin IV provides a novel pathway for disulphide formation in the endoplasmic reticulum. The EMBO journal 2010;29:4185-4197
23. Jang I, Pottekat A, Poothong J, Yong J, Lagunas-Acosta J, Charbono A, Chen Z, Scheuner DL, Liu M, Itkin-Ansari P: PDIA1/P4HB is required for efficient proinsulin maturation and ß cell health in response to diet induced obesity. eLife 2019;8:e44528
24. Wang YJ, Schug J, Won KJ, Liu C, Naji A, Avrahami D, Golson ML, Kaestner KH: Single-Cell Transcriptomics of the Human Endocrine Pancreas. Diabetes 2016;65:3028-3038
25. Mehmeti I, Lortz S, Elsner M, Lenzen S: Peroxiredoxin 4 improves insulin biosynthesis and glucose-induced insulin secretion in insulin-secreting INS-1E cells. Journal of Biological Chemistry 2014;289:26904-26913
26. Wood ZA, Schröder E, Robin Harris J, Poole LB: Structure, mechanism and regulation of peroxiredoxins. Trends in Biochemical Sciences 2003;28:32-40
27. Ghiasi SM, Dahlby T, Andersen CH, Haataja L, Petersen S, Omar-Hmeadi M, Yang M, Pihl C, Bresson SE, Khilji MS: Endoplasmic Reticulum Chaperone Glucose-Regulated Protein 94 Is Essential for Proinsulin Handling. Diabetes 2019;68:747-760
28. Pottekat A, Becker S, Spencer KR, Yates III JR, Manning G, Itkin-Ansari P, Balch WE: Insulin biosynthetic interaction network component, TMEM24, facilitates insulin reserve pool release. Cell reports 2013;4:921-930
29. Iuchi Y, Okada F, Tsunoda S, Kibe N, Shirasawa N, Ikawa M, Okabe M, Ikeda Y, Fujii J: Peroxiredoxin 4 knockout results in elevated spermatogenic cell death via oxidative stress. Biochemical Journal 2009;419:149-158
30. Caillard A, Sadoune M, Cescau A, Meddour M, Gandon M, Polidano E, Delcayre C, Da Silva K, Manivet P, Gomez A-M: QSOX1, a novel actor of cardiac protection upon acute stress in mice. Journal of molecular and cellular cardiology 2018;119:75-86
31. Day AM, Brown JD, Taylor SR, Rand JD, Morgan BA, Veal EA: Inactivation of a peroxiredoxin by hydrogen peroxide is critical for thioredoxin-mediated repair of oxidized proteins and cell survival. Molecular cell 2012;45:398-408
32. Ding Y, Yamada S, Wang K-Y, Shimajiri S, Guo X, Tanimoto A, Murata Y, Kitajima S, Watanabe T, Izumi H: Overexpression of peroxiredoxin 4 protects against high-dose streptozotocin-induced diabetes by suppressing oxidative stress and cytokines in transgenic mice. Antioxidants & redox signaling 2010;13:1477-1490
33. Palande K, Roovers O, Gits J, Verwijmeren C, Iuchi Y, Fujii J, Neel BG, Karisch R, Tavernier J, Touw IP: Peroxiredoxin-controlled G-CSF signalling at the endoplasmic reticulum–early endosome interface. J Cell Sci 2011;124:3695-3705
34. El Eter E, Al-Masri A: Peroxiredoxin isoforms are associated with cardiovascular risk factors in type 2 diabetes mellitus. Brazilian Journal of Medical and Biological Research 2015;48:465-469
35. Nabeshima A, Yamada S, Guo X, Tanimoto A, Wang KY, Shimajiri S, Kimura S, Tasaki T, Noguchi H, Kitada S, Watanabe T, Fujii J, Kohno K, Sasaguri Y: Peroxiredoxin 4 protects against nonalcoholic steatohepatitis and type 2 diabetes in a nongenetic mouse model. Antioxid Redox Signal 2013;19:1983-1998
36. Hutt DM, Balch WE: Expanding proteostasis by membrane trafficking networks. Cold Spring Harbor perspectives in biology 2013;5:a013383

37. Powers ET, Balch WE: Diversity in the origins of proteostasis networks—a driver for protein function in evolution. Nature reviews Molecular cell biology 2013;14:237
38. Chawade A, Alexandersson E, Levander F: Normalyzer: a tool for rapid evaluation of normalization methods for omics data sets. Journal of proteome research 2014;13:3114-3120
39. Choi H, Larsen B, Lin Z-Y, Breitkreutz A, Mellacheruvu D, Fermin D, Qin ZS, Tyers M, Gingras A-C, Nesvizhskii AI: SAINT: probabilistic scoring of affinity purification–mass spectrometry data. Nature methods 2011;8:70
40. Clough T, Thaminy S, Ragg S, Aebersold R, Vitek O: Statistical protein quantification and significance analysis in label-free LC-MS experiments with complex designs. BMC bioinformatics 2012;13:S6
41. Tripathi S, Pohl MO, Zhou Y, Rodriguez-Frandsen A, Wang G, Stein DA, Moulton HM, DeJesus P, Che J, Mulder LC: Meta-and orthogonal integration of influenza "OMICs" data defines a role for UBR4 in virus budding. Cell host & microbe 2015;18:723-735
42. Kuleshov MV, Jones MR, Rouillard AD, Fernandez NF, Duan Q, Wang Z, Koplev S, Jenkins SL, Jagodnik KM, Lachmann A: Enrichr: a comprehensive gene set enrichment analysis web server 2016 update. Nucleic acids research 2016;44:W90-W97
43. Uhlén M, Fagerberg L, Hallström BM, Lindskog C, Oksvold P, Mardinoglu A, Sivertsson Å, Kampf C, Sjöstedt E, Asplund A: Tissue-based map of the human proteome. Science 2015;347:1260419
44. Alanis-Lobato G, Andrade-Navarro MA, Schaefer MH: HIPPIE v2. 0: enhancing meaningfulness and reliability of protein–protein interaction networks. Nucleic acids research 2016:gkw985
45. Vanunu O, Magger O, Ruppin E, Shlomi T, Sharan R: Associating genes and protein complexes with disease via network propagation. PLoS computational biology 2010;6:e1000641
46. Huang S-sC, Fraenkel E: Integrating proteomic, transcriptional, and interactome data reveals hidden components of signaling and regulatory networks. Sci Signal 2009;2:ra40-ra40
47. Loguercio S: Network-Augmented Genomic Analysis (NAGA) applied to cystic fibrosis studies. F1000Research 2015;4
48. Shannon P, Markiel A, Ozier O, Baliga NS, Wang JT, Ramage D, Amin N, Schwikowski B, Ideker T: Cytoscape: a software environment for integrated models of biomolecular interaction networks. Genome research 2003;13:2498-2504
49. Liu M, Haataja L, Wright J, Wickramasinghe NP, Hua Q-X, Phillips NF, Barbetti F, Weiss MA, Arvan P: Mutant INS-gene induced diabetes of youth: proinsulin cysteine residues impose dominant-negative inhibition on wild-type proinsulin transport. PloS one 2010;5:e13333

A reference map of the human proinsulin biosynthetic interaction network

Figures and Supp

Figure 1. Identification of Proinsulin Interactions in Human Islets

A

ID	Age	Ethnicity	Gender	COD	BMI	HbA1C
I-020	57	African American	F	ICH-stroke	23.1	5.0%
I-007	56	Caucasian	F	ICH-stroke	23.1	5.4%
I-338	41	African American	M	ICH-stroke	24.6	5.4%
I-315	51	Caucasian	F	CVA-stroke	21.0	5.3%
I-259	37	Hispanic	M	CVA-ICH-stroke	25.4	5.5%
I-232	36	Hispanic	F	ICH-stroke	24.6	4.8%

B

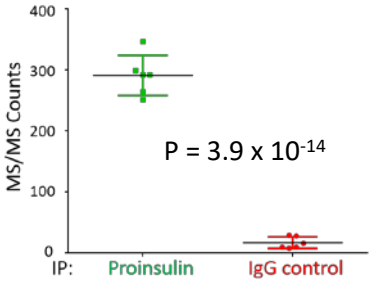

C

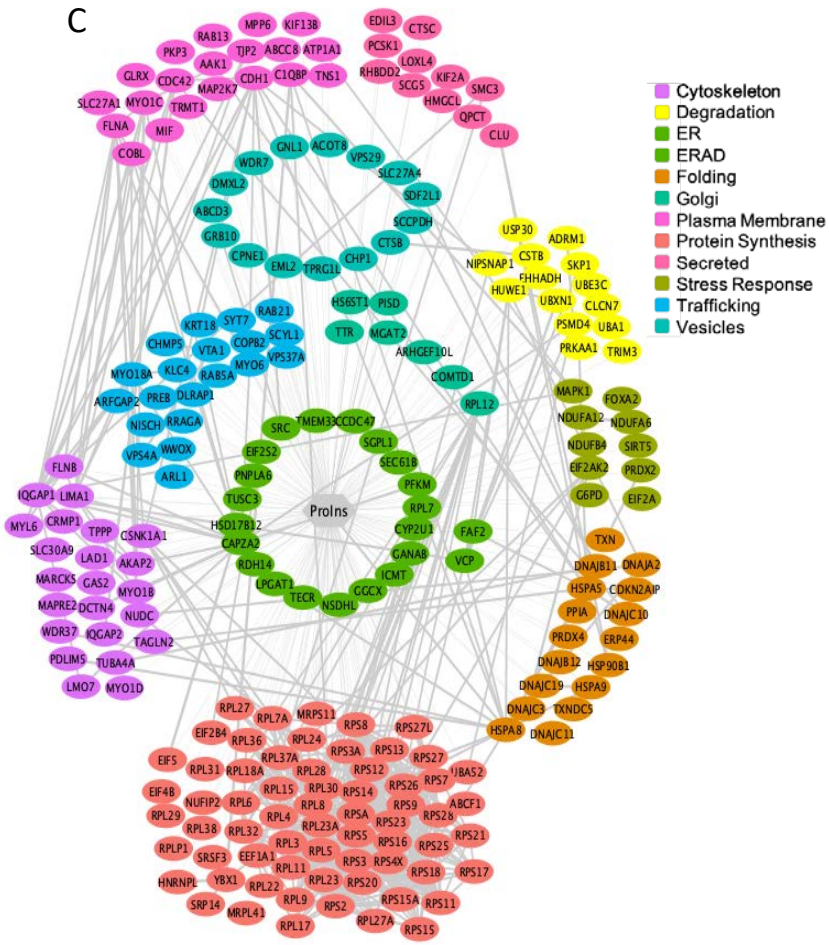

Figure 2 - PRDX4 is a robust proinsulin interactor and is induced by loss of PDI1

A

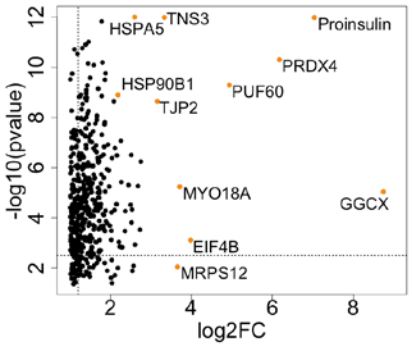

B

Family	Gene name	Folding factor	Name	Proins IP/Control IP p-value
			Chaperones	
Hsp90	HSP90B1	Grp94	Endoplasmin	1.3×10^{-9}
Hsp70	HSPA5	BiP	78 kDa glucose-regulated protein	0
	HSPA8			3.6×10^{-6}
			Cochaperones	
Hsp40	DNAJB11	ERDJ3	DnaJ homolog subfamily B member 11	1.2×10^{-6}
	DNAJB12		DnaJ homolog subfamily B member 12	5.3×10^{-3}
	DNAJC10	ERDJ5	DnaJ homolog subfamily C member 10	5.5×10^{-6}
	DNAJC3	ERDJ6	DnaJ homolog subfamily C member 3	5.3×10^{-5}
			Oxidoreductases	
PDI	P4HB	PDI	Protein disulfide-isomerase	3.3×10^{-4}
	DUOX2		Dual Oxidase 2	6.3×10^{-7}
	ERP44	ERp44	Endoplasmic reticulum resident protein 44	1.9×10^{-6}
Sulfydryl oxidase	ERO1B	Ero1β	ERO1-like protein beta	9.9×10^{-4}
PDI-Erv	QSOX1	QSOX1	Sulfhydryl oxidase 1	0.05
Thioredoxin	TXN		Thioredoxin	4.5×10^{-3}
	TNXL1		Thioredoxin like 1	7.2×10^{-3}
	TXNDC5	ERp46	Thioredoxin domain-containing protein 5	7.2×10^{-10}
Peroxiredoxin	PRDX4	PrxIV	Peroxiredoxin-4	4.9×10^{-11}
			ERAD	
	VCP	p97	Valosin containing protein	9×10^{-4}
	FAF2	UBXD8		5.8×10^{-6}

C

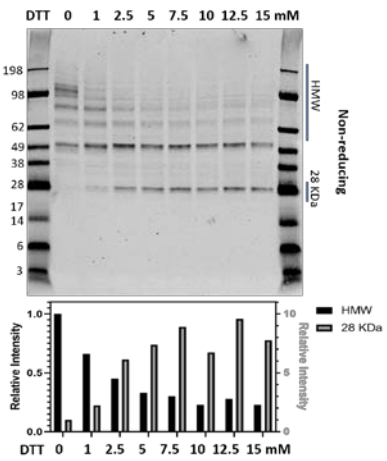

D

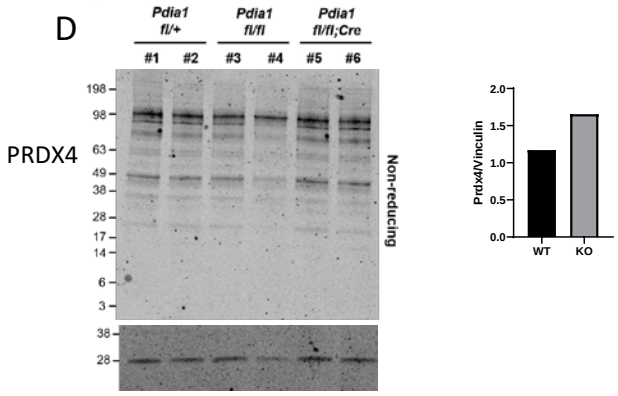

E

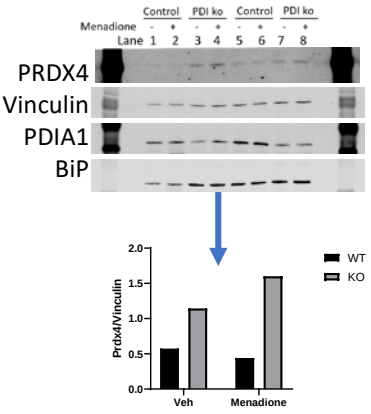

F

Non-reducing

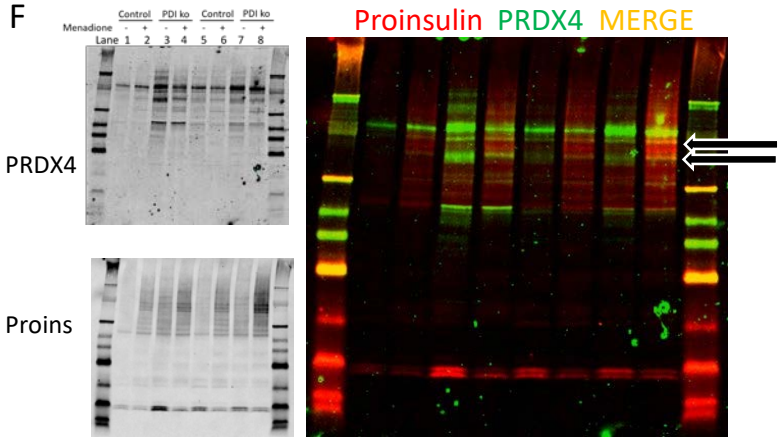

Figure 3 - Loss of PRDX4 exacerbates proinsulin misfolding induced by BiP cleavage, oxidative stress in MIN6 cell lines

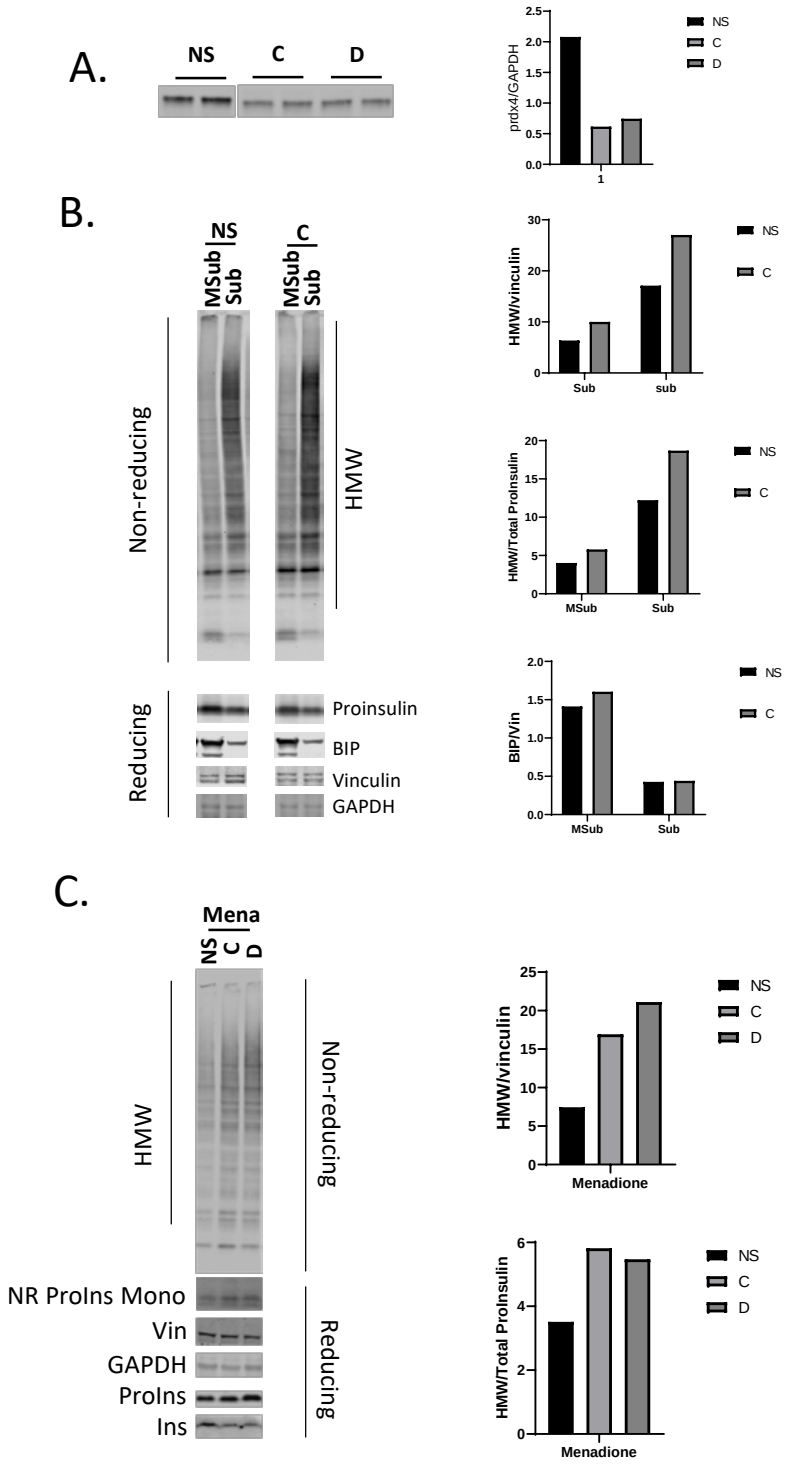

Figure 4 - Oxidant (Menadione) treatment of human islets induces proinsulin misfolding, increased proinsulin:BiP interactions and PRDX4 sulfonylation

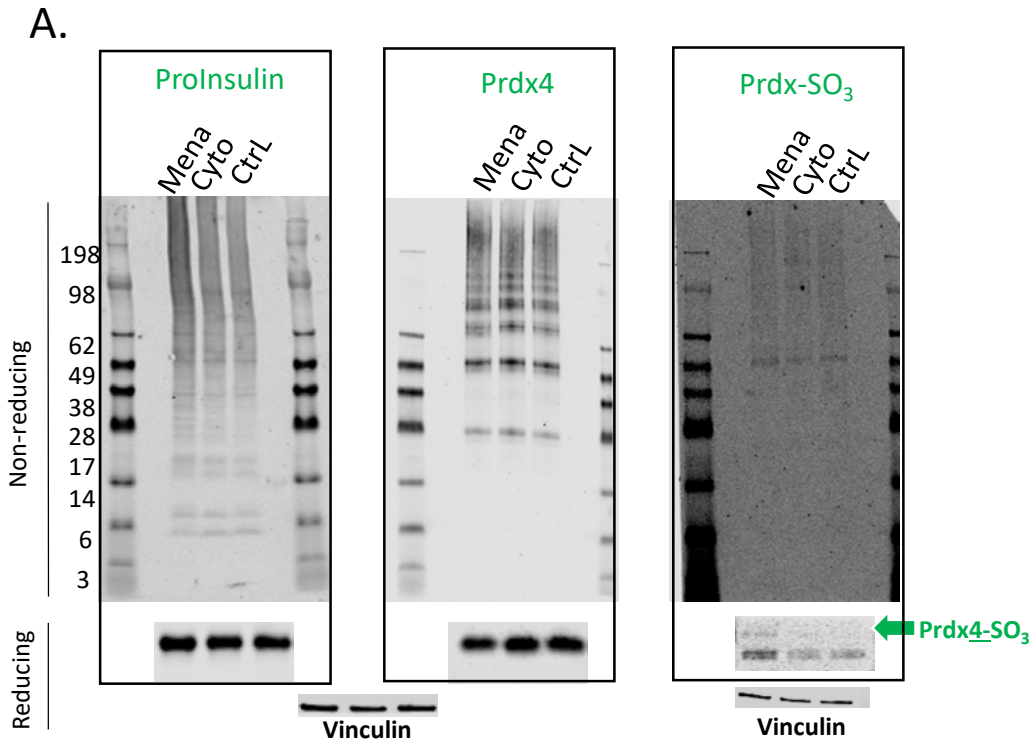

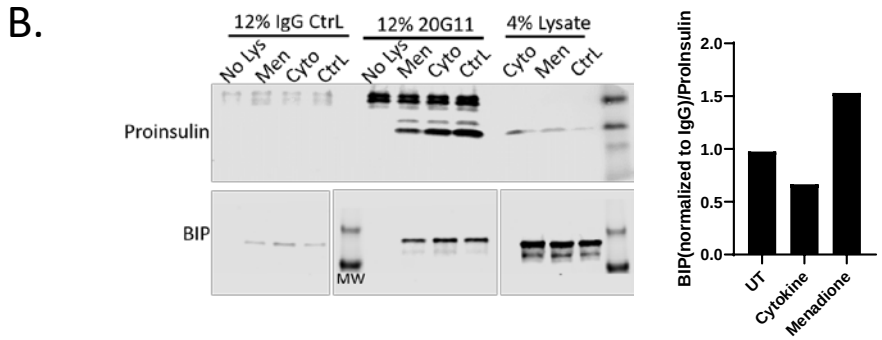

Figure 5 - T2D islets trend to high molecular proinsulin complexes relative to monomer and exhibit increased PRDX4 sulfonylation

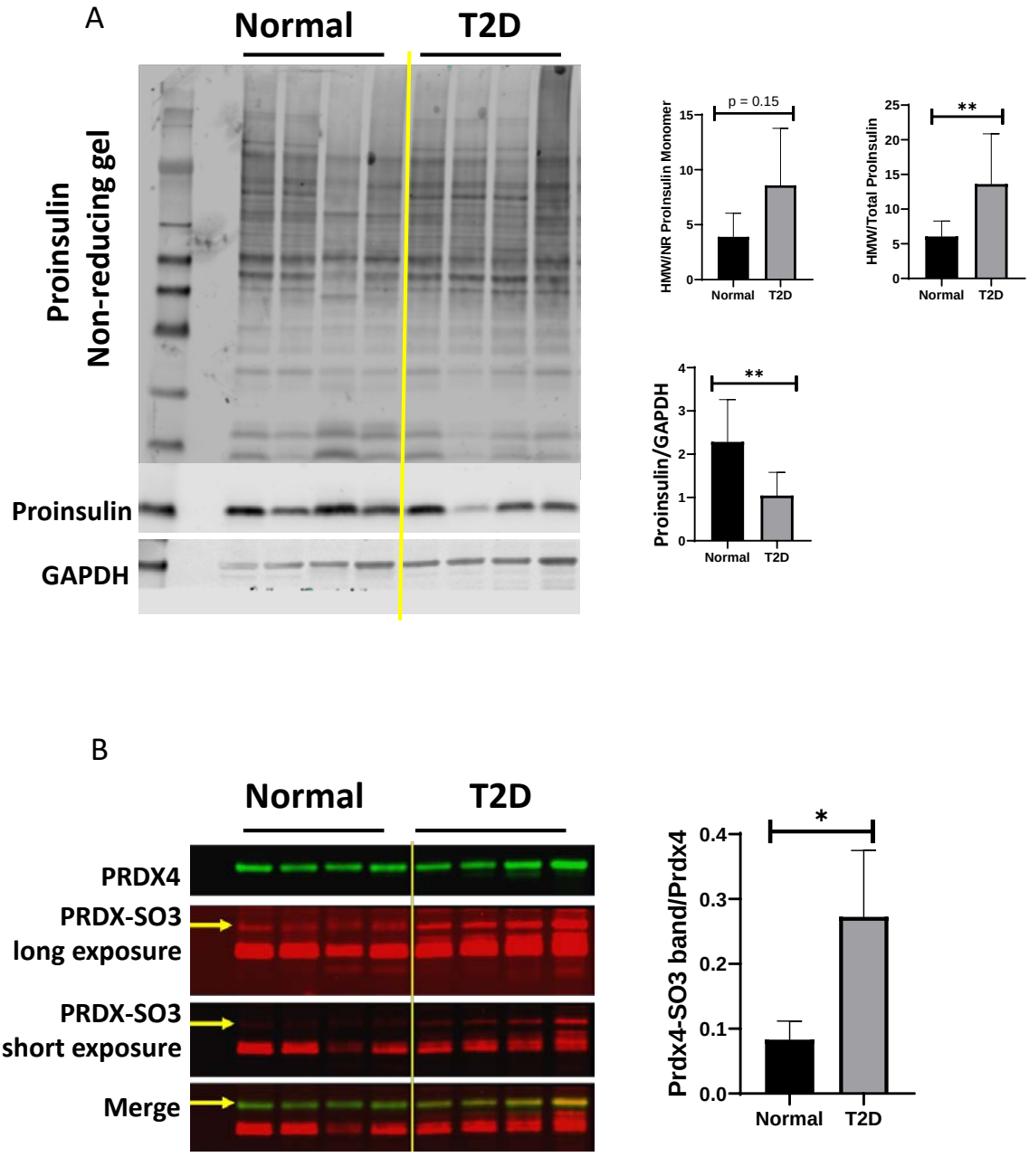

Supplemental Figures

Supp. Fig. 1. Antibody Generation and Validation

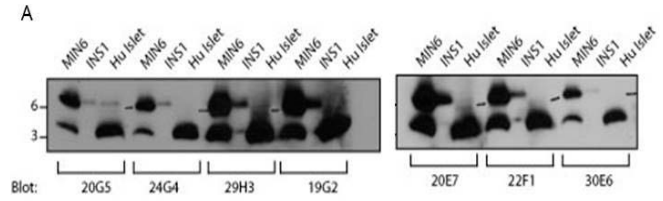

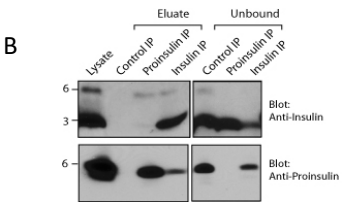

20G11

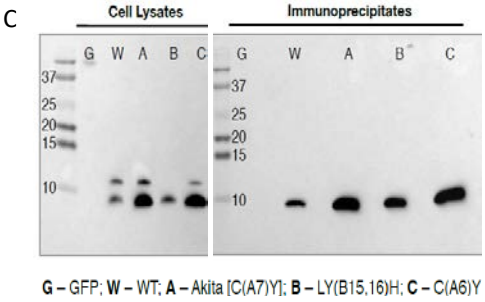

G – GFP; **W** – WT; **A** – Akita [C(A7)Y]; **B** – LY(B15,16)H; **C** – C(A6)Y

20G11

Supp Fig. 2 Comparison of Label Free and TMT analysis of an Islet prep (HP-15157-01)

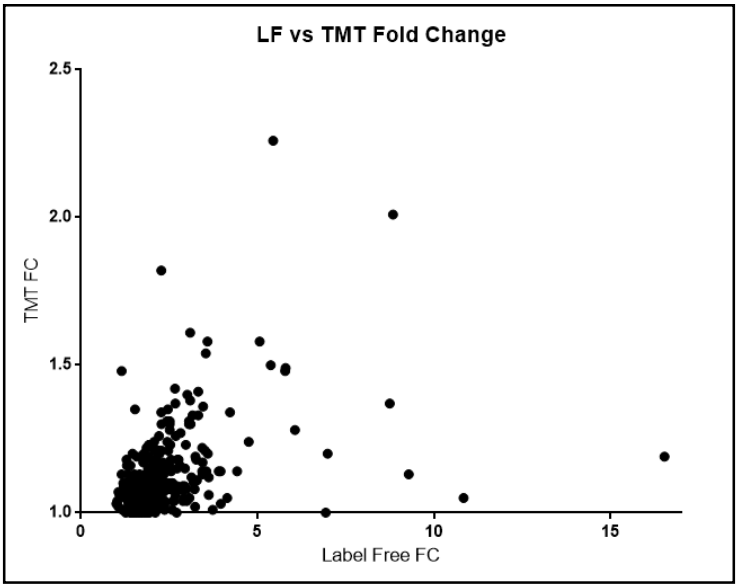

Supp. Fig. 3. Validate MS/MS Interactions by AP-western blot showed Proins interacts with MYO18A, BIP, ERDJ3, ERDJ5, ERGIC1 GRP94, PRDX4, QSOX1

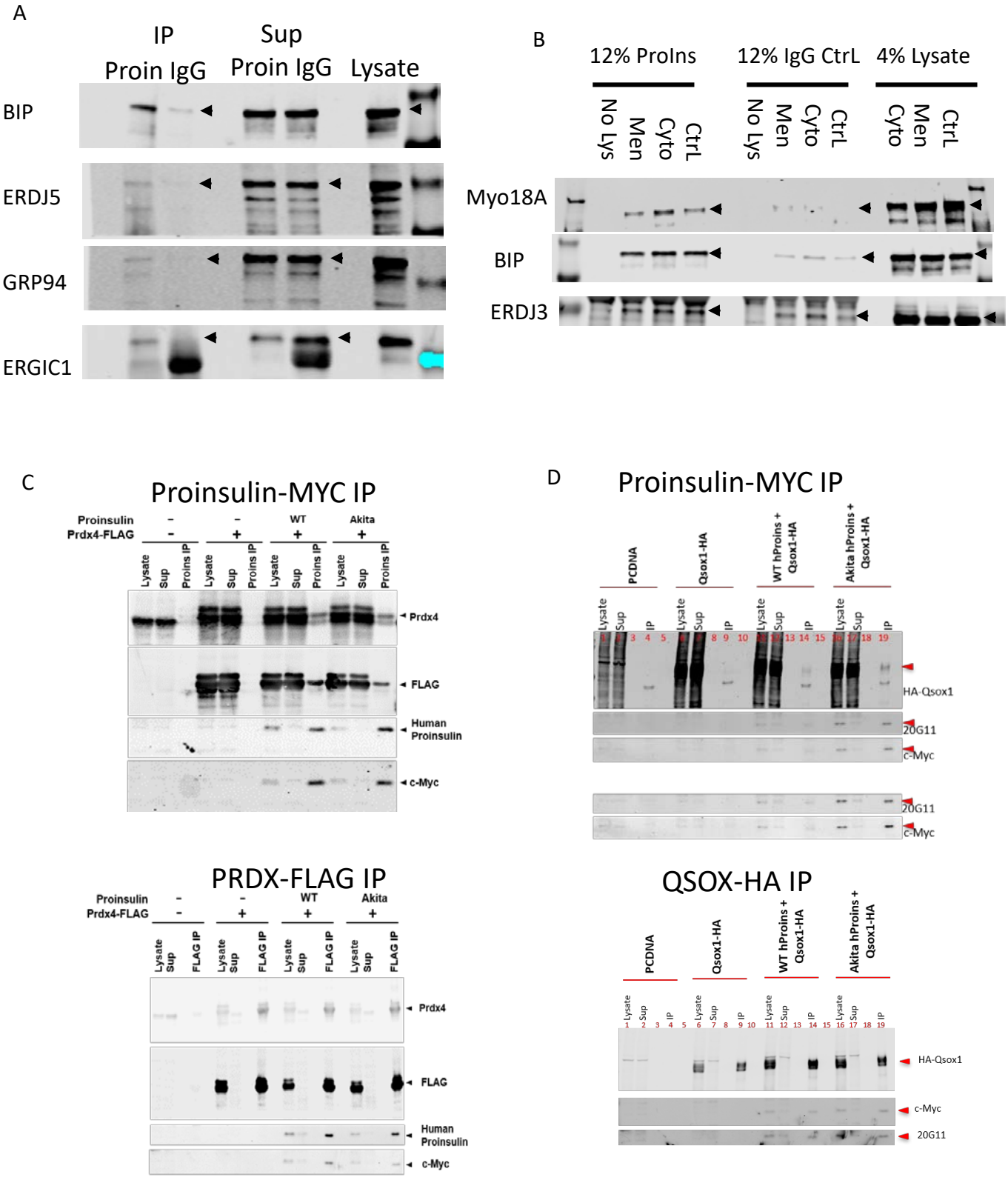

Supp. Fig. 4. PRDX4 expression vs PDX1 expression in human beta cell single cell RNAseq